PROCEEDINGS OF SCIENCE

Measurements of jet fragmentation and jet substructure with ALICE

Markus Fasel for the ALICE Collaboration*
Oak Ridge National Laboratory, Oak Ridge, Tennessee, United States
E-mail: markus.fasel@cern.ch

We discuss the latest results from jet fragmentation and jet substructure measurements performed with the ALICE experiment in proton-proton and heavy-ion collisions in a wide range of jet transverse momentum. The jet production cross sections and cross section ratios for different jet resolution parameters will be shown in a wide range of p_{T}. Results will be compared to next-to-leading order pQCD calculations.

7th Annual Conference on Large Hadron Collider Physics - LHCP2019
20-25 May, 2019
Puebla, Mexico

*Speaker.

PoS(LHCP2019)212

1. Introduction

Jet substructure measurements at low transverse momentum p_{T} allow to constrain various perturbative and non-perturbative effects contributing to jet production, such as hadronization, perturbative radiation and the underlying event. For example the measurement of the jet cross section for various jet resolution parameters R and the ratios of cross sections, in particular for $p_{\mathrm{T}} < 100$ GeV/c show different sensitivity to the various effects [1]. In addition, the large datasets obtained with LHC Run2 allow for more differential studies. This is used in the measurement of the groomed momentum fraction z_{g} using the SoftDrop algorithm [2, 3], defined as

$$z_{\mathrm{g}} = \frac{min(p_{\mathrm{T},1}, p_{\mathrm{T},2})}{p_{\mathrm{T},1} + p_{\mathrm{T},2}} > z_{cut}\,\theta^{\beta} \tag{1.1}$$

with $p_{\mathrm{T},1}$ and $p_{\mathrm{T},2}$ being the p_{T} of the hardest and second hardest subjet. The level of grooming is controlled by the parameters z_{cut} and β. The observable is selected as it is closely related to the QCD splitting function at leading order [1]. No p_{T}-dependence is expected. The difference between the parton and the reconstructed jet momentum is expected to increase as $\log(R)$ for perturbative radiation, to decrease as $1/R$ due to hadronization effects and to increase as $\sim R^2$ due to the contribution from the underlying event [1]. In heavy-ion collisions the groomed momentum fraction is sensitive to effects from the hot and dense medium.

Jets are reconstructed using the anti-k_{T} algorithm [4] from the FastJet package [5] employing the E scheme recombination. Clustering is done for track-based jets using tracks reconstructed in the ALICE tracking detectors, requiring a minimum constituent p_{T} of 150 MeV/c. For fully reconstructed jets clusters in the electromagnetic calorimeter with energy larger than 300 MeV are included in the jet reconstruction.

The data used for the measurement in pp collisions at $\sqrt{s} = 13$ TeV was collected in 2016 and 2017, consisting of a min. bias dataset with $L_{\mathrm{int}} = 11.5$ nb^{-1} and a jet-triggered dataset based on energy deposition in the electromagnetic calorimeter with $L_{\mathrm{int}} = 4$ pb^{-1}. For the measurements in heavy-ion collisions the data was collected at $\sqrt{s_{\mathrm{NN}}} = 2.76$ TeV in 2011 and consists of 16M central collisions.

In heavy-ion collisions jet reconstruction is affected by the particles from the underlying event. Therefore observables with low sensitivity to the background, like jet-hadron correlations [6] are preferential. For substructure measurements the effect of the uncorrelated background can be handled in the detector response. For this PYTHIA events [7, 8] are embedded into heavy-ion events, and the effect of the background is estimated and subtracted using area based [9] or constituent based [10] subtraction methods.

2. Measurement of the jet production in pp collisions at $\sqrt{s} = 13$ TeV

The p_{T}-differential cross section of jet production is measured for different jet radii between $R = 0.2$ and $R = 0.6$ for 20 GeV/c $< p_{\mathrm{T}} <$ 320 GeV/c (Fig. 1 (left)). The comparison to POWHEG+PYTHIA6 [11, 12, 13] is shown in Fig. 2 for $R = 0.2$ (left) and $R = 0.4$ (right). POWHEG calculations use $\mu_R = \mu_F = 1$. Calculations are in good agreement with the measured production cross sections. The ratios of the differential jet production cross section for jets with

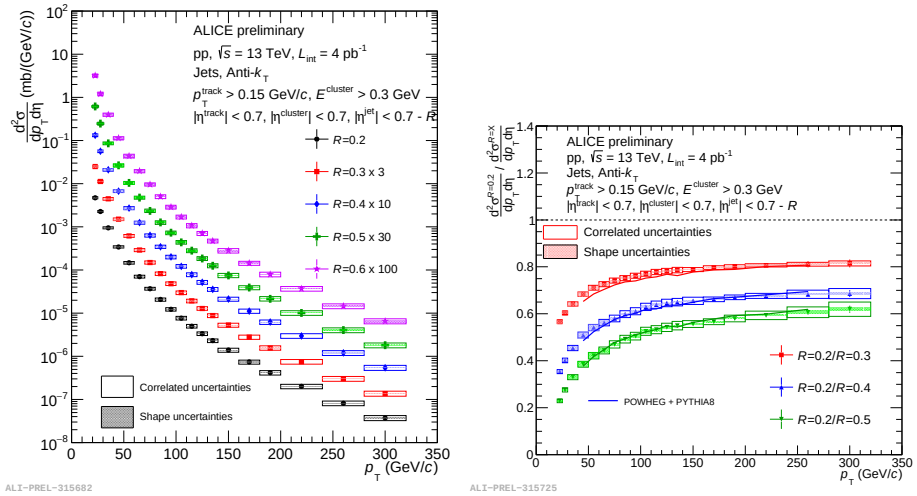

Figure 1: Left: p_{T}-differential jet production cross section in pp collisions at $\sqrt{s} = 13$ TeV for different R. Right: Ratios of jet production cross sections for jets with $R = 0.2$ to the cross section for various R. Lines indicate calculations using POWHEG+PYTHIA6.

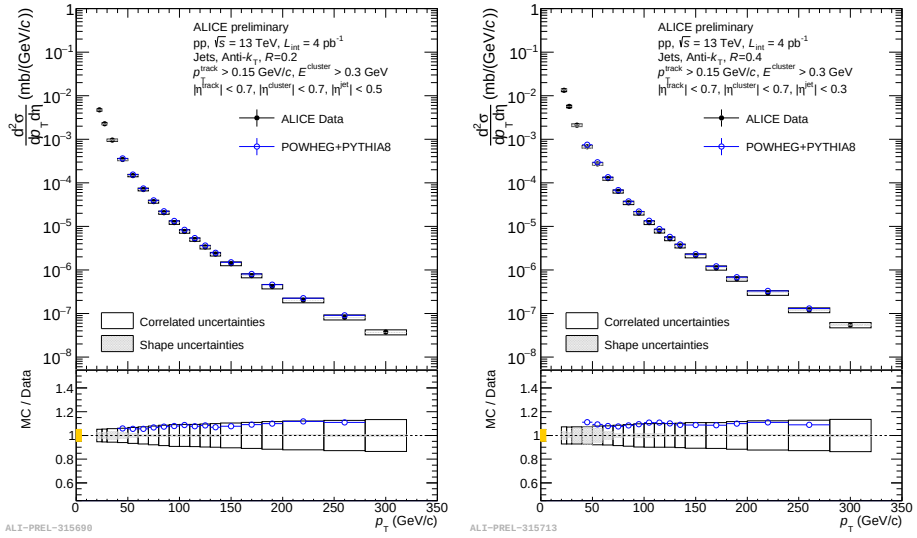

Figure 2: p_{T}-differential jet production cross section for jets with $R = 0.2$ (left) and $R = 0.4$ (right) compared to POWHEG+PYTHIA6 ($\mu_R = \mu_F = 1$).

$R = 0.2$ to the cross section for various R is shown in Fig. 1 (right) for $R = 0.3$ to $R = 0.6$ in the same p_{T} range. As many of the systematic uncertainties cancel in the ratios they can be measured with a higher precision. The cross section ratios are well-described by POWHEG+PYTHIA6. A good agreement with POWHEG+PYTHIA6 has also been found in cross section measurements of track-based jets and fully reconstructed jets at lower centre-of-mass energies [14, 15, 16].

3. Measurement of the groomed momentum fraction z_g in pp and heavy-ion collisions

In pp collisions at $\sqrt{s}$ = 13 TeV the groomed momentum fraction z_{g} has been measured for jets with 30 GeV/c < p_{T} < 200 GeV/c for various ranges in p_{T}. Jets were reclustered with the Cambridge/Aachen algorithm. The SoftDrop parameters β = 0 and z_{g} = 0.1 were used. No underlying event subtraction has been applied as the grooming already removes soft components from the underlying event. The distributions are unfolded back to particle level using a 2-dimensional unfolding based on the Bayesian method [17]. The response matrices have been obtained using a full detector simulation based on GEANT3 [18] of pp events at the same centre-of-mass energy generated with PYTHIA8 [8].

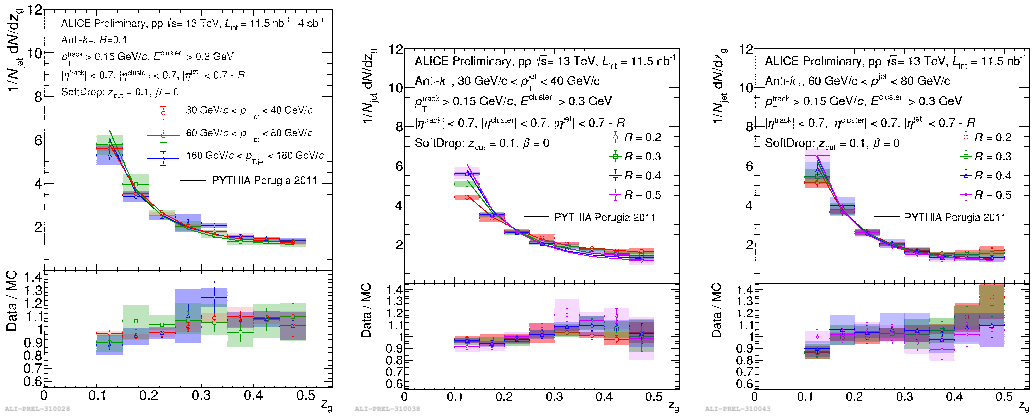

Figure 3: Left: z_{g}-differential per-jet yield for jets with R=0.4 for different bins in p_{T} (left), jets with different R for 30 GeV/c < p_{T} < 40 GeV/c (middle), and jets with different R for 60 GeV/c < p_{T} < 80 GeV/c (right). Lines indicate calculations with the PYTHIA event generator using the Perugia 0 tune [19].

Fig. 3 (left) shows the z_g- differential jet yield for jets with R = 0.4 for 30 GeV/c < p_{T} < 40 GeV/c, 60 GeV/c < p_{T} < 80 GeV/c, and 160 GeV/c < p_{T} < 180 GeV/c. Results agree within the uncertainties, indicating no p_{T}-dependence of the z_{g} for jets with large resolution parameter. In the middle and right panel the z_{g}-differential yield of jets is plotted for different R from R = 0.2 to R = 0.4 for jets with 30 GeV/c < p_{T} < 40 GeV/c (middle) and 60 GeV/c < p_{T} < 80 GeV/c (right). For jets with lower p_{T} a difference in the z_{g}-differential yield for different R is observed, tending towards more symmetric splitting for jets with smaller R. For jets with higher p_{T} no dependence of the z_{g} on R is observed. The trend is well reproduced by PYTHIA6 using the Perugia 0 tune.

In Pb-Pb collisions the z_{g}-differential yield of track based jets was measured at $\sqrt{s_{\mathrm{NN}}}$ = 2.76 TeV for jets with R = 0.4 and 80 GeV/c < p_{T} < 120 GeV/c [20]. Fig. 4 shows the z_{g}- differential yields for strongly collimated jets with ΔR < 0.1, where ΔR is the distance between the subjets, and jets with ΔR > 0.2. For the comparison to the vacuum PYTHIA events were embedded into PbPb events in order to account for effects from the underlying background. While no modification can be observed for very collimated subjets, for jets with larger ΔR a suppression of jets with symmetric splittings with an enhancement of untagged jets can be observed.

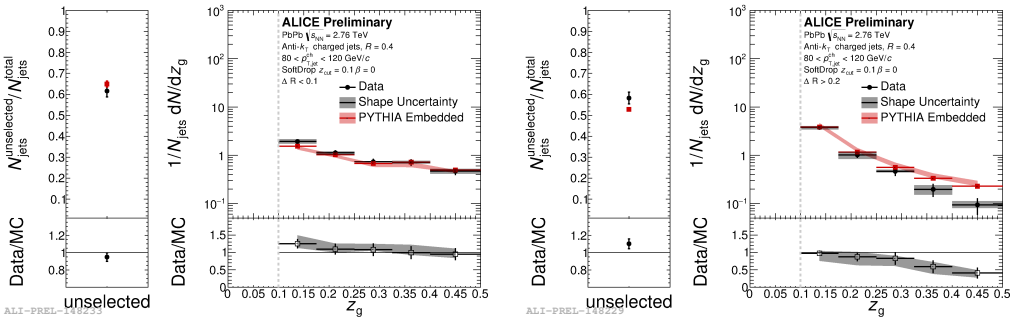

Figure 4: z_g-differential yield of track-based jets with 80 GeV/c $< p_T <$ 120 GeV/c and $R = 0.4$. [20] Left: jets with $\Delta R < 0.1$. Right: jets with $\Delta R > 0.2$. Red bands indicating the distributions from PYTHIA events embedded into heavy-ion collisions.

4. Outlook

The study of jet substructure can be generalized by varying the grooming conditions or looking at all splittings and constructing the Lund plane [21]. The Lund plane is obtained directly from the QCD kernel. Recent studies [22] show that different regions in the Lund plane are sensitive to different effects, among them medium-induced radiation and coherent radiation. A precise measurement of the Lund plane in heavy-ion collisions will allow to provide further constraints on the different effects contributing to jet modification in the hot and dense medium.

References

[1] M. Dasgupta, F. A. Dreyer, G. P. Salam and G. Soyez, *Inclusive jet spectrum for small-radius jets*, *JHEP* **06** (2016) 057 [1602.01110].

[2] A. J. Larkoski, S. Marzani, G. Soyez and J. Thaler, *Soft Drop*, *JHEP* **05** (2014) 146 [1402.2657].

[3] J. M. Butterworth, A. R. Davison, M. Rubin and G. P. Salam, *Jet substructure as a new Higgs search channel at the LHC*, *Phys. Rev. Lett.* **100** (2008) 242001 [0802.2470].

[4] M. Cacciari, G. P. Salam and G. Soyez, *The anti-k_t jet clustering algorithm*, *JHEP* **04** (2008) 063 [0802.1189].

[5] M. Cacciari, G. P. Salam and G. Soyez, *FastJet User Manual*, *Eur. Phys. J.* **C72** (2012) 1896 [1111.6097].

[6] ALICE collaboration, J. Adam et al., *Measurement of jet quenching with semi-inclusive hadron-jet distributions in central Pb-Pb collisions at* $\sqrt{s_{\rm NN}} = 2.76$ *TeV*, *JHEP* **09** (2015) 170 [1506.03984].

[7] T. Sjostrand, S. Mrenna and P. Z. Skands, *PYTHIA 6.4 Physics and Manual*, *JHEP* **05** (2006) 026 [hep-ph/0603175].

[8] T. SjÃűstrand, S. Ask, J. R. Christiansen, R. Corke, N. Desai, P. Ilten et al., *An Introduction to PYTHIA 8.2*, *Comput. Phys. Commun.* **191** (2015) 159 [1410.3012].

[9] G. Soyez, G. P. Salam, J. Kim, S. Dutta and M. Cacciari, *Pileup subtraction for jet shapes*, *Phys. Rev. Lett.* **110** (2013) 162001 [1211.2811].

[10] P. Berta, M. Spousta, D. W. Miller and R. Leitner, *Particle-level pileup subtraction for jets and jet shapes*, *JHEP* **06** (2014) 092 [1403.3108].

[11] S. Frixione, P. Nason and C. Oleari, *Matching NLO QCD computations with Parton Shower simulations: the POWHEG method*, *JHEP* **11** (2007) 070 [0709.2092].

[12] S. Alioli, P. Nason, C. Oleari and E. Re, *A general framework for implementing NLO calculations in shower Monte Carlo programs: the POWHEG BOX*, *JHEP* **06** (2010) 043 [1002.2581].

[13] S. Alioli, K. Hamilton, P. Nason, C. Oleari and E. Re, *Jet pair production in POWHEG*, *JHEP* **04** (2011) 081 [1012.3380].

[14] ALICE collaboration, J. Mulligan, *Inclusive jet measurements in pp and Pb-Pb collisions with ALICE*, *PoS* **HardProbes2018** (2019) 080 [1812.07681].

[15] ALICE collaboration, S. Acharya et al., *Measurement of charged jet cross section in pp collisions at* $\sqrt{s} = 5.02$ *TeV*, 1905.02536.

[16] ALICE collaboration, S. Acharya et al., *Charged jet cross section and fragmentation in proton-proton collisions at* $\sqrt{s} = 7$ *TeV*, *Phys. Rev.* **D99** (2019) 012016 [1809.03232].

[17] G. D'Agostini, *A multidimensional unfolding method based on bayes' theorem*, *Nuclear Instruments and Methods in Physics Research Section A: Accelerators, Spectrometers, Detectors and Associated Equipment* **362** (1995) 487 .

[18] R. Brun, F. Bruyant, M. Maire, A. McPherson and P. Zanarini, *GEANT3*, .

[19] P. Z. Skands, *Tuning Monte Carlo Generators: The Perugia Tunes*, *Phys. Rev.* **D82** (2010) 074018 [1005.3457].

[20] ALICE collaboration, S. Acharya et al., *Exploration of jet substructure using iterative declustering in pp and Pb-Pb collisions at LHC energies*, 1905.02512.

[21] B. Andersson, G. Gustafson, L. Lonnblad and U. Pettersson, *Coherence Effects in Deep Inelastic Scattering*, *Z. Phys.* **C43** (1989) 625.

[22] H. A. Andrews et al., *Novel tools and observables for jet physics in heavy-ion collisions*, 1808.03689.